Phase Equilibria in the Ln_2O_3-V_2O_3-V_2O_5 (Ln=Dy and Ho) Systems at 1200 °C

Kenzo KITAYAMA* and Takashi KATSURA
Department of Chemistry, Faculty of Science, Tokyo Institute of Technology, Ookayama, Meguro-ku, Tokyo 152
(Received October 4, 1983)

Phase equilibria in the systems, Dy_2O_3-V_2O_3-V_2O_5 and Ho_2O_3-V_2O_3-V_2O_5, were established at 1200 °C by changing the oxygen partial pressure from 4.32 to −7.50 Pa in terms of $\log P_{O_2}$. In both systems, Ln_2O_3, $LnVO_4$, $LnVO_3$, V_nO_{2n-1}(n=2—7), VO_2, and $Ln_8V_2O_{17}$($4Ln_2O_3 \cdot V_2O_5$) are stable, and compounds with mole ratio Ln_2O_3/V_2O_5=5/1 are not stable under the present experimental conditions. On the basis of the established phase diagrams, the standard Gibbs energies of reactions, (1) $3\,Dy_2O_3+2\,DyVO_3+O_2=Dy_8V_2O_{17}$, (2) $DyVO_3+1/2\,O_2=DyVO_4$, (3) $3\,Ho_2O_3+2\,HoVO_3+O_2=Ho_8V_2O_{17}$, and (4) $HoVO_3+1/2\,O_2=HoVO_4$, were determined to be −278, −123.8, −277, and −122.4 kJ, respectively. $LnVO_4$, $Ln_8V_2O_{17}$, V_2O_3, and VO_2 have nonstoichiometric compositions. $\Delta G°$ values for reactions (2) and (4) fit well on the linear line presented by us.

The phase equilibria in the Ln_2O_3-V_2O_3-V_2O_5 systems[1-8] at 1200 °C were established by changing the oxygen partial pressures from 4.32 (air) to −7.50 or −8.00 Pa in terms of $\log P_{O_2}$. These established phase diagrams showed different patterns one another because of the differences of compounds coexisting under the experimental conditions although systems with Gd_2O_3[4] and Eu_2O_3[8] showed a similar pattern. Besides, the standard Gibbs energies of reactions found in the established diagrams and crystallographic data of the compounds presented for the systems have been obtained. It has also been established that the relationship between the ionic radius and $\Delta G°$ of reaction, $LnVO_3+1/2\,O_2=LnVO_4$, is linear provided that the lanthanoid elements can be divided into two groups.

In the present study, Dy_2O_3 and Ho_2O_3 were chosen as Ln_2O_3. In the Dy_2O_3-V_2O_5 and Ho_2O_3-V_2O_5 systems, compounds with mole ratio Ln_2O_3/V_2O_5 4/1 and 5/1 were stable[9] in the air from 600 to 1500 °C in addition to the well-known $LnVO_4$. So new types of phase equilibria will be expected.

Only one report was available about Dy_2O_3-V_2O_3 system,[10] in which one compound $DyVO_3$ with the congruent melting point at 2100 °C was found and it is nonstoichiometric toward V_2O_3 side in the temperature range from about 1800 to 2000 °C. The Ho_2O_3-V_2O_3 system has not been completely studied on account of the instability of V_2O_3 in the air, but $HoVO_3$ is well-known as a stable phase.

The crystallographic properties of $DyVO_3$, $HoVO_3$, $DyVO_4$, and $HoVO_4$ were investigated by many researchers.[11-14]

The objectives of the present study are: (1) preparation of the detailed phases diagrams of both systems at 1200 °C in order to determine the stable compounds under the present experimental conditions, (2) calculation of the standard Gibbs energies of reactions appeared in the established phase diagrams, and (3) examination of the fitness of present data on the linear relationship between the standard Gibbs energies of reactions and the ionic radius of the lanthanoid elements.

Experimental

Analytical grades of Dy_2O_3 (99.9%), Ho_2O_3 (99.9%), and V_2O_5, which was made by heating NH_4VO_3 of the guaranteed grade at 500 °C in the air for about 24 h, were used as the starting materials. Desired Dy_2O_3/V_2O_5 and Ho_2O_3/V_2O_5 mole ratios of samples were obtained by mixing appropriate quantities throughly in an agate motar under ethyl alcohol. The mixtures were treated by the procedures described in the previous paper.[1] The apparatus and procedures for controlling the oxygen partial pressures and keeping a constant temperature, the method of thermogravimetry, the criterion for an equilibrium establishment, the method of measurement of the actual oxygen partial pressure, and the method of chemical analysis are the same as those reported in the previous papers.[1,15-19]

Results and Discussion

Phase Equilibria. It was ascertained by the preliminary studies that Dy_2O_3 is stable under the present experimental ranges of the oxygen partial pressure. Seven samples with Dy_2O_3/V_2O_5 mole ratios 85/15, 8/2, 7/3, 65/35, 1, 35/65, and 15/85 were prepared to be used in the thermogravimetric experiments. The thermogravimetric results for three samples with mole ratios 85/15, 7/3, and 35/65 are shown in Fig. 1 as representative. In Fig. 1 the ordinate is the oxygen partial pressure represented in $\log P_{O_2}$ in the Pa unit and the abscissa is the composition shown by W_{O_2}/W_T, where W_{O_2} is the weight gain of the samples from the reference weight at $\log P_{O_2}$=−7.50, which is a point in the oxygen partial pressures where Dy_2O_3, $DyVO_3$, and V_2O_3 are stable, and W_T is the total weight increase of samples which might get if V_2O_3 in the samples at the reference state changed to V_2O_5 in the higher oxygen partial pressures. The W_{O_2}/W_T ratio was usually shown in the range from 0.995 to 1.00 in the air. Figure 1 shows the different patterns one another, and in the oxygen partial pressure range from $\log P_{O_2}$=−7.50 to −4.85 (Fig. 1a) the weight change was not observed. The value of $\log P_{O_2}$=−4.85 is the oxygen partial presure of the gas phase in equilibrium with the phase assemblages R+A_2+

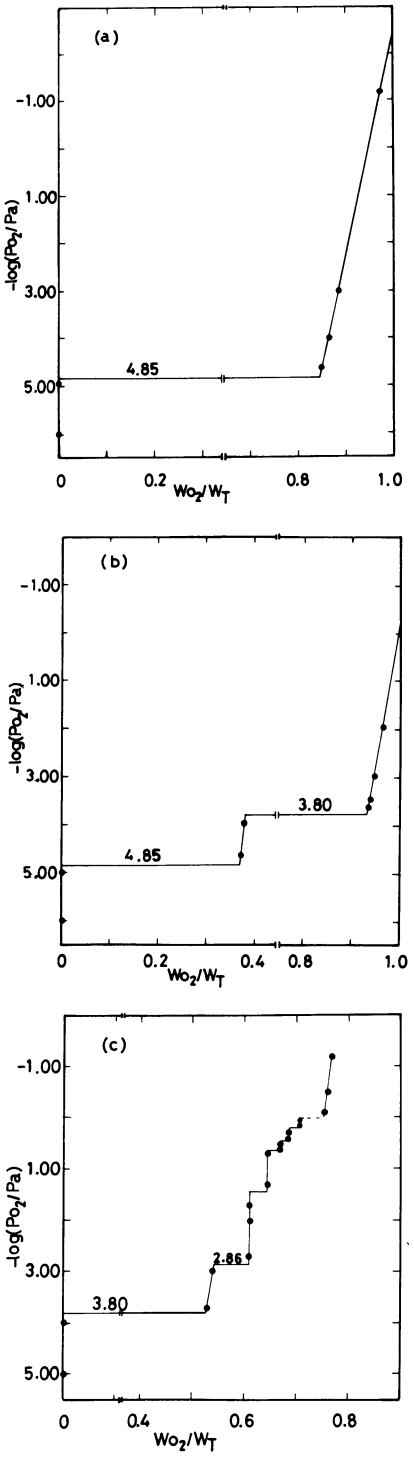

Fig. 1. The relationships between $-\log(P_{O_2}/\text{Pa})$ and the compositions, W_{O_2}/W_T, of the samples.
(a) $Dy_2O_3/V_2O_5=85/15$, (b) $Dy_2O_3/V_2O_5=7/3$, (c) $Dy_2O_3/V_2O_5=35/65$.

C which symboles will be shown in Table 2. In the range higher than $\log P_{O_2}=-4.85$, the weight changes linearly with the change in oxygen partial pressures. Figure 1b shows two oxygen partial pressures, −4.85 and −3.80 in $\log P_{O_2}$, in equilibrium. The latter corresponds to that of Reaction (2) in Table 4, and Fig. 1c have six oxygen partial pressures in equilibrium

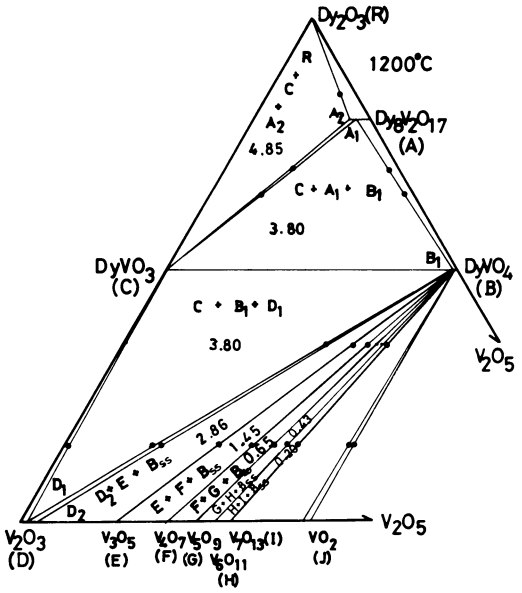

Fig. 2. Phase equilibria in the Dy_2O_3-V_2O_3-V_2O_5 system at 1200 °C. Numerical values in the three solid phases regions are the oxygen partial pressures in equilibrium in $-\log P_{O_2}$. Symbols are the same as those in Table 2.

in which five values correspond to those of the reactions in the V-O system.[1)]

In Table 1 the results of identification of phases are shown. In the first column are shown the compositions of the starting materials in mole%, in the second the experimental conditions of the oxygen partial pressure in terms of $\log P_{O_2}$ in Pa, in the third the experimental durations in hours, and in the last the phases that were found in the respective quenched samples using X-ray powder diffractometer with Cu $K\alpha$ radiation.

Based upon the above thermogravimetric results and the results of identification of phases, a phase diagram of the system can be constructed and is shown in Fig. 2. The following phases are stable; $V_nO_{2n-1}(n=2—7)$, VO_2, Dy_2O_3, $DyVO_4$, $DyVO_3$, and $Dy_8V_2O_{17}(4Dy_2O_3 \cdot V_2O_5)$. The compound $5Dy_2O_3 \cdot V_2O_5$ reported by Brusset *et al.*[9)] as the stable phase was not found.

The stability of Ho_2O_3 under the present experimental conditions was confirmed by preliminary experiments. Seven samples with Ho_2O_3/V_2O_5 mole ratios 85/15, 8/2, 7/3, 6/4, 1, 35/65, and 15/85 have also been used in the thermogravimetric experiments. The value of $\log P_{O_2}=-7.50$ was selected as the reference oxygen partial pressure by the similar reason as described above. In Fig. 3 the relationships between the oxygen partial pressure and the composition of samples are shown as those in Fig. 1 with the representative samples having mole ratios 85/15, 6/4, and 15/85. Figure 3 shows similar patterns to Fig. 1.

Quenched samples were used for the identification of phases and the phases were identified by X-ray powder diffractometer with Cu $K\alpha$ radiation. The results are shown in Table 1 together with those of the Dy_2O_3-V_2O_3-V_2O_5 system. Figure 4 was depicted by using

above experimental results as those in Fig. 2. Figures. 2 and 4 give similar patterns each other. In addition to the seven oxides in the V_2O_3–V_2O_5 system, Ho_2O_3, $HoVO_4$, $HoVO_3$, and $Ho_8V_2O_{17}(4Ho_2O_3 \cdot V_2O_5)$ are stable. These phase diagrams are very simple having only one compound between Ln_2O_3 and $LnVO_4$. This type of the phase diagram was found in the systems of Eu, Gd, and Er. It was very interesting that

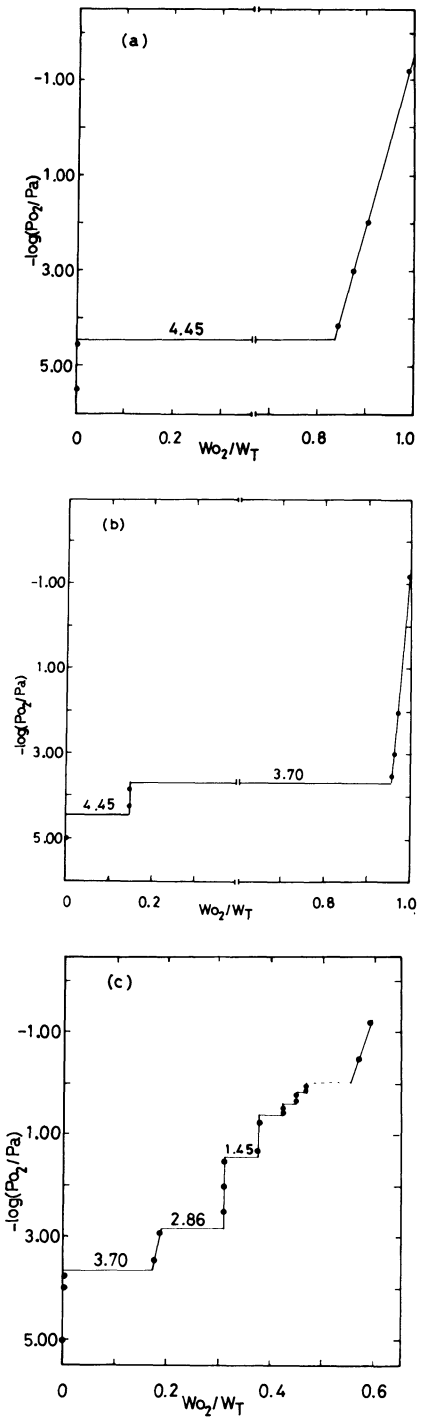

Fig. 3. The relationships between $-\log(P_{O_2}/\text{Pa})$ and the compositions, W_{O_2}/W_T of samples.
(a) $Ho_2O_3/V_2O_5=85/15$, (b) $Ho_2O_3/V_2O_5=6/4$, (c) $Ho_2O_3/V_2O_5=15/85$.

Table 1. Identification of phases

Starting materials mol%		$-\log(P_{O_2}/\text{Pa})$	Time h	Phases
Dy_2O_3	V_2O_5			
85	15	7.50	8	$Dy_2O_3+DyVO_3$
		5.00	27	$Dy_2O_3+DyVO_3$
		4.50	22	$Dy_2O_3+Dy_8V_2O_{17}$
		−4.32	63	$Dy_2O_3+Dy_8V_2O_{17}$
65	35	7.50	8	$Dy_2O_3+DyVO_3$
		5.00	27	$Dy_2O_3+DyVO_3$
		4.50	22	$DyVO_3+Dy_8V_2O_{17}$
		2.50	27	$DyVO_4+Dy_8V_2O_{17}$
		−4.32	63	$DyVO_4+Dy_8V_2O_{17}$
35	65	7.50	8	$DyVO_3+V_2O_3$
		4.50	22	$DyVO_3+V_2O_3$
		3.30	28	$DyVO_4+V_2O_3$
		2.00	27	$DyVO_4+V_3O_5$
		1.00	28	$DyVO_4+V_4O_7$
		0.55	39	$DyVO_4+V_5O_9$
		0.35	41	$DyVO_4+V_6O_{11}$
		0.10	56	$DyVO_4+V_7O_{13}$
		−0.55	39	$DyVO_4+VO_2$
15	85	7.50	8	$DyVO_3+V_2O_3$
		4.50	22	$DyVO_3+V_2O_3$
		3.30	28	$DyVO_4+V_2O_3$
		2.00	27	$DyVO_4+V_3O_5$
		1.00	28	$DyVO_4+V_4O_7$
		0.55	39	$DyVO_4+V_5O_9$
		0.35	41	$DyVO_4+V_6O_{11}$
		0.10	56	$DyVO_4+V_7O_{13}$
		−0.55	39	$DyVO_4+VO_2$
Ho_2O_3	V_2O_5			
85	15	6.00	24	$Ho_2O_3+HoVO_3$
		4.00	24	$Ho_2O_3+Ho_8V_2O_{17}$
		−4.32	63	$Ho_2O_3+Ho_8V_2O_{17}$
70	30	6.00	24	$Ho_2O_3+HoVO_3$
		3.90	24	$Ho_2O_3+Ho_8V_2O_{17}$
		3.00	24	$HoVO_4+Ho_8V_2O_{17}$
		−4.32	63	$HoVO_4+Ho_8V_2O_{17}$
35	65	6.00	24	$HoVO_3+V_2O_3$
		4.00	24	$HoVO_3+V_2O_3$
		3.00	26	$HoVO_4+V_2O_3$
		2.00	26	$HoVO_4+V_3O_5$
		1.00	48	$HoVO_4+V_4O_7$
		0.55	48	$HoVO_4+V_5O_9$
		0.30	47	$HoVO_4+V_6O_{11}$
		0.10	48	$HoVO_4+V_7O_{13}$
		−0.50	32	$HoVO_4+VO_2$
15	85	6.00	24	$HoVO_3+V_2O_3$
		4.00	24	$HoVO_3+V_2O_3$
		3.00	26	$HoVO_4+V_2O_3$
		2.00	26	$HoVO_4+V_3O_5$
		1.00	48	$HoVO_4+V_4O_7$
		0.55	48	$HoVO_4+V_5O_9$
		0.30	47	$HoVO_4+V_6O_{11}$
		0.10	48	$HoVO_4+V_7O_{13}$
		−0.50	32	$HoVO_4+VO_2$

these elements are located in the middle of the lanthanoid.

$DyVO_4$, $HoVO_4$, $Dy_8V_2O_{17}$, and $Ho_8V_2O_{17}$ have nonstoichiometric compositions, and the relationships between the oxygen partial pressure and the compositions were obtained as follows: $N_O/N_B=4.23\times10^{-3}\log P_{O_2}-1.38\times10^{-4}$ for $DyVO_4$, $N_O/N_L=8.80\times10^{-3}\log P_{O_2}+6.37\times10^{-3}$ for $HoVO_4$, $N_O/N_A=0.045\log P_{O_2}-0.098$ for $Dy_8V_2O_{17}$, and $N_O/N_K=0.079\log P_{O_2}-0.023$ for $Ho_8V_2O_{17}$, where N_O is the mole fraction of oxygen atom in the compounds and N_A, N_B, N_K, and N_L are the mole fractions of the $Dy_8V_2O_{17}$, $DyVO_4$, $Ho_8V_2O_{17}$, and $HoVO_4$ components in the compounds, respectively.

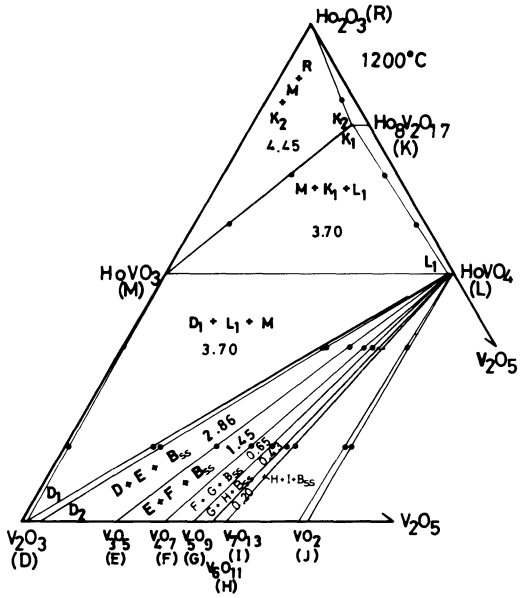

Fig. 4. Phase equilibria in the Ho_2O_3-V_2O_3-V_2O_5 system at 1200 °C. Numerical values in the three solid phases regions are the oxygen partial pressures in equilibrium in $-\log P_{O_2}$. Symbols are the same as those in Table 2.

Table 2 lists the compositions of the compounds at various oxygen partial pressures, stability ranges of the compounds in terms of $\log P_{O_2}$, the symbols of the compounds, and the activities of the components described above. The activities of the components in the solid solutions were calculated by means of the Gibbs-Duhem equation with the data of thermogravimetry, for example N_O/N_A *vs.* $\log P_{O_2}$ described above. A detailed method of the calculation has been discussed in the previous paper.[18]

Lattice constants of the compounds $DyVO_3$, $DyVO_4$, $Dy_8V_2O_{17}$, $HoVO_3$, $HoVO_4$, and $Ho_8V_2O_{17}$ are tabulated in Table 3. Present values are in good agreement

Table 2. Compositions, symbols, stability ranges in the oxygen partial pressures, and activities of component in the solid solutions

Component	Composition	Symbol	$-\log(P_{O_2}/\mathrm{Pa})$	$-\log a_i$
$Dy_8V_2O_{17}$	$Dy_8V_2O_{17.0}$	A	-2.1[a)]$-$$-4.32$	0.55
	$Dy_8V_2O_{16.73}$	A_1	3.80	0.15
	$Dy_8V_2O_{16.69}$	A_2	4.85	0
$DyVO_4$	$DyVO_{4.00}$	B	0.0[a)]$-$$-4.32$	0.016
	$DyVO_{3.98}$	B_1	3.80	0
$Ho_8V_2O_{17}$	$Ho_8V_2O_{17.0}$	K	-0.3[a)]$-$$-4.32$	0.45
	$Ho_8V_2O_{16.7}$	K_1	3.70	0.13
	$Ho_8V_2O_{16.6}$	K_2	4.45	0
$HoVO_4$	$HoVO_{4.00}$	L	0.7[a)]$-$$-4.32$	0.020
	$HoVO_{3.97}$	L_1	3.70	0

a) These values were obtained by extrapolating the thermogravimetric results.

Table 3. Cell dimensions of compounds

Sample	$-\log(P_{O_2}/\mathrm{Pa})$	a/Å	b/Å	c/Å	β/°	V/Å^3	Ref
$DyVO_3$	7.50	5.311±0.003	5.618±0.003	7.602±0.004		226.8±0.2	
	5.00	5.305±0.002	5.613±0.002	7.603±0.002		226.4±0.2	
		5.299	5.594	7.593		225.1	11
		5.302	5.602	7.601			12
$DyVO_4$	−4.32	7.157±0.002		6.317±0.002		323.6±0.2	
	3.50	7.157±0.002		6.315±0.002		323.5±0.2	
		7.1434		6.313			13
$Dy_8V_2O_{17}$	−4.32	10.69 ±0.05	8.81 ±0.14	15.75 ±0.12	99.1±0.5	1460±20	
	4.50	10.71 ±0.08	8.65 ±0.08	15.48 ±0.28	98.8±0.5	1420±30	
$HoVO_3$	4.00	5.283±0.002	5.609±0.002	7.580±0.002		224.6±0.2	
	6.00	5.277±0.002	5.597±0.002	7.579±0.002		223.8±0.2	
		5.276	5.592	7.576		223.5	11
$HoVO_4$	−4.32	7.129±0.002		6.293±0.002		319.8±0.2	
	3.50	7.129±0.002		6.300±0.004		320.2±0.3	
		7.1214		6.2926			14
$Ho_8V_2O_{17}$	−4.32	10.69 ±0.10	8.43 ±0.05	15.22 ±0.36	98.4±0.7	1360±35	
	4.00	10.65 ±0.08	8.61 ±0.07	15.49 ±0.28	99.0±0.5	1400±30	

TABLE 4. THE STANDARD GIBBS ENERGIES OF REACTIONS

Reaction	$-\log(P_{O_2}/Pa)$	$\frac{-\Delta G^\circ}{kJ}$
(1) $3\,Dy_2O_3+2\,DyVO_3+O_2=Dy_8V_2O_{17}$	4.85±0.05	278±1
(2) $DyVO_3+1/2\,O_2=DyVO_4$	3.80±0.03	123.8±0.5
(3) $3\,Ho_2O_3+2\,HoVO_3+O_2=Ho_8V_2O_{17}$	4.45±0.07	277±2
(4) $HoVO_3+1/2\,O_2=HoVO_4$	3.70±0.03	122.4±0.5

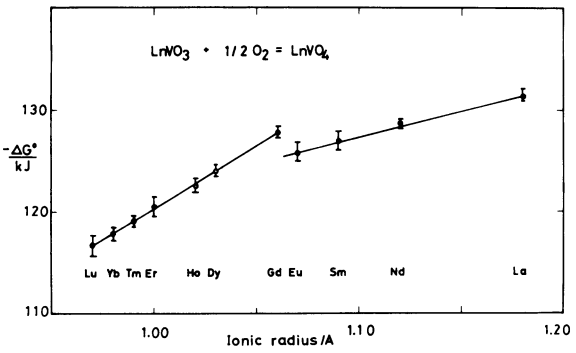

Fig. 5. The relationship between the ionic radius of lanthanoid elements with eight coordination and the ΔG° values of reaction, $LnVO_3+1/2\,O_2=LnVO_4$.

with those quoted in the Table. There are no considerable differences in values of the samples which were prepared under the different conditions of oxygen partial pressures. Lattice constants of $Dy_8V_2O_{17}$ and $Ho_8V_2O_{17}$ were determined with the data of $4\,Tm_2O_3 \cdot V_2O_5$.[20] Experimental errors are still large compared with the data of other compounds.

Calculation of the Standard Gibbs Energies of Reactions. On the basis of the present phase equilibria, the standard Gibbs energies of the reactions appeared in the systems, except for the partial system of V_2O_3–V_2O_5, can be calculated by an equation, $\Delta G^\circ=-RT\ln K$, where R is the gas constant, T, the absolute temperature, and K, the equilibrium constant of each reaction. Chemical reactions appeared in the phase diagrams, the oxygen partial pressures in equilibrium for each reaction, and ΔG° values obtained are shown in Table 4. Activities of each component in solid solutions, which are necessary for the calculation, are given in Table 2.

The Relationship between ΔG° and Ionic Radius. In the series of Ln_2O_3–V_2O_3–V_2O_5 system, the common reaction, $LnVO_3+1/2\,O_2=LnVO_4$, appeares in all the systems. It is very interesting to correlate the ΔG° values of reactions with some properties of lanthanoid elements. In a previous report,[7] we have graphically presented the linear relationship between ΔG° values and the ionic radius of lanthanoid elements with eight coordination, provided that the lanthanoid series was subdivided into two groups. The present program is to ascertain whether or not the data obtained in the present systems fit well to the previous linear relation. The values of the present systems are plotted in Fig. 5 with open circles. These circles are well fit on the line which has been drawn using the data of previous results of another systems.

References

1) K. Kitayama and T. Katsura, *Bull. Chem. Soc. Jpn.*, **50**, 889 (1977).
2) K. Kitayama and T. Katsura, *Bull. Chem. Soc. Jpn.*, **51**, 1358 (1978).
3) K. Kitayama, T. Sugihara, and T. Katsura, *Bull. Chem. Soc. Jpn.*, **52**, 458 (1979).
4) K. Kitayama and T. Katsura, *Bull. Chem. Soc. Jpn.*, **55**, 1820 (1982).
5) K. Kitayama, D. Zoshima, and T. Katsura, *Bull. Chem. Soc. Jpn.*, **56**, 689 (1983).
6) K. Kitayama, C. Mizokuchi, and T. Katsura, *Bull. Chem. Soc. Jpn.*, **56**, 695 (1983).
7) K. Kitayama and T. Katsura, *Bull. Chem. Soc, Jpn.*, **56**, 1084 (1983).
8) K. Kitayama, H. Sou, and T. Katsura, *Bull. Chem. Soc. Jpn.*, **56**, 3415 (1983).
9) H. Brusset, F. Madaule-Aubry, B. Blanck, J. P. Glaziou, and J. P. Laude, *Can. J. Chem.*, **49**, 3700 (1971).
10) A. K. Molodkin, V. N. Belan, Yu. E. Bogatov, and V. I. Moskalenko, *Zh. Neorg. Khim.*, **27**, 1033 (1982).
11) G. J. McCarthy, C. A. Sipe, and K. E. McIlvried, *Mater. Res. Bull.*, **9**, 1279 (1974).
12) B. Reuter, *Col. Int. C. N. R. S.*, 1053 (1965).
13) J. C. P. D. S. Card No. 16-870.
14) J. C. P. D. S. Card No. 15-764.
15) T. Katsura and H. Hasegawa, *Bull. Chem. Soc. Jpn.*, **40**, 561 (1967).
16) N. Kimizuka and T. Katsura, *J. Solid State Chem.*, **13**, 176 (1975).
17) T. Katsura and A. Muan, *Trans. AIME*, **230**, 77 (1964).
18) N. Kimizuka and T. Katsura, *J. Solid State Chem.*, **15**, 151 (1975).
19) N. Kimizuka and T. Katsura, *Bull. Chem. Soc. Jpn.*, **47**, 1801 (1974).
20) H. Brusset, R. Mahe, and J. P. Laude, *Bull. Soc. Chim. Fr.*, **1973**, 495.